Open Archive TOULOUSE Archive Ouverte (OATAO)

OATAO is an open access repository that collects the work of Toulouse researchers and makes it freely available over the web where possible.

This is an author-deposited version published in: http://oatao.univ-toulouse.fr/
Eprints ID: 16754

Any correspondence concerning this service should be sent to the repository administrator: staff-oatao@listes-diff.inp-toulouse.fr

A novel design and control solution for an aircraft sidestick actuator based on Halbach permanent magnet machine

S. Fergani[1], J.F. Allias[1], Y. Briere[1], F. Defay[1]

[1] *Université de Toulouse, ISAE-SUPAERO (Institut Supérieur de l'Aéronautique et de l'Espace), DCAS, 10 Avenue Edouard Belin, BP 54032-31055 Toulouse Cedex, France. Corresponding author:*
soheib.fergani@isae.fr

Abstract:
This paper is concerned with the design and control of a new sidestick actuators used to handle a civilian aircraft behaviour. Indeed, a discrete robust adaptive sliding mode control for a new designed aircraft sidestick based on synchronous Halbach permanent magnet machine.

The main objective is to provide a new design structure and a control solution that ensures maintaining high performance specifications for the actuator and respects the set of constraints required by the considered aeronautical application. Indeed, this study achieved in a partnership with an industrial center of excellence for Fly by Wire Cockpit Controls (side sticks, rudder controls, thrust controls), proposes a novel design that enhances the characteristics of the actuator's structure and the human machine interface between the pilot and the aircraft. Then, a new control strategy is proposed to optimize the efficiency of this actuator for the considered application. It is based on a discrete optimal adaptive sliding mode control considering time delays and uncertainties in the model by using a delay ahead predictor. The proposed strategy combines an optimal sliding mode surface with the delay ahead predictor in an adaptive control structure. Indeed, a varying parameter is used to achieve an "on-line" adaption to the varying level of disturbances that affects the system. Then, since the sidestick actuator is designed to handle an aircraft displacement, the proposed control strategy is designed for position tracking. Simulations performed on the previously designed actuator prove the efficiency of the proposed technological solution for aircraft position control.

Keywords: Actuator design, structure optimisation, discrete system, , linear quadratic control, sliding mode control, adaptive control.

1. INTRODUCTION

During the last decades, the evolution of the aeronautical technologies has provided huge advances in the design and control of the aircraft and aerospace vehicles. Indeed, the continuously increasing interest of the big industrial groups in this field and the increasing number of the air transportation companies has led the academic community to develop several studies that aim to provide novel solutions for the encountered problems. Indeed, a lot of innovations have been provided to optimize and manage the behaviour of these aerodynamical vehicles (especially aircrafts) and to improve their characteristics and performances.

One of the most important issues is to improve the pilot handling of the aircraft using flight control surfaces (see MORGAN (1991)). First, the mechanical passive sidestick system were conventionally used for the fly-by-wire as explained in Wyllie (1988).

Usually, two passive sidesticks are available in the cockpit (see Fig. 1) to create force feedback depending on the displacement angle of the stick compared to the natural resting position: on the left side for the pilot and for the right side for the copilot.

The following two Fly-by-wire systems are the most used in the aeronautical industry: electro-hydraulic ones allow to adapt the aircraft behaviour to flight envelope through a variable stiffness (see Navarro (1997), and Karpenko and Sepehri (2009)) and the electric systems (see Brière and Traverse (1993))that provide excellent characteristics regarding force feed back (with high bandwidth allowing to change the stiffness and adapt the aircraft behaviour) and also new functions that ensure haptic feedback.

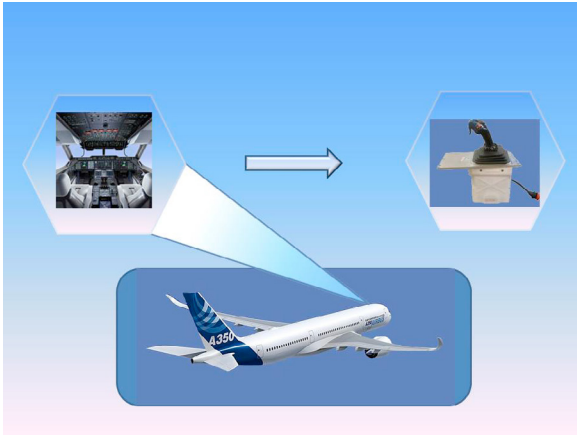Due to the increasing size of the aircrafts, the passive

Fig. 1. Aircraft cockpit

sidesticks can not handle properly the flight control surfaces. This has led to the use of the "active sidestick" that uses motors, electronics and high bandwidth closed loop control systems to overcome this issue. It allows to handle the oversized aeronautical vehicle with less pilot effort while providing better haptic sensations (Hanke and Herbst (1999), Hegg et al. (1995)).

Recently, it has been proven that haptic sensation of the pilot can be enhanced thanks to the active sidestick technology. Some of these works have focused on teleomerization and UAV control as in Lam et al. (2008), Gandhi et al. (2014) and Zanlucchi et al. (2014).

The control of this type of sidesticks has been subject to several studies. Many control approaches have provided some solutions to enhance the use of the active sidesticks actuators for aerodynamical vehicles handling.

One interesting control approach is the linear state feedback control since it has the full flexibility of shaping the dynamics of the closed loops system to meet the desired specification (Carriere et al. (2010)). But, the problem is once the external disturbances and/or parameter uncertainties exist, the desired responses may not be obtained (lack of robustness), (see Kumar et al. (2008)). Also, another problem is to handle the time delays that occurs on the considered models.

To overcome this problematic, some robust control strategies have been proposed to handle the disturbances and the parameter uncertainties (Bhattacharyya et al. (1995), Adams et al. (2012). It can be understood that each one of the proposed strategies focuses on only some robustness issues and mostly aren't able to handle the time delays.

In this paper, a new discrete adaptive optimal sliding mode robust control strategy based on LQR gain, sliding surface and adaptation parameter. Indeed, this parameter is achieved as follows: the LQR optimal approach used to shape the actuator dynamics and meet the requirement of the performance index in nominal conditions for the reaching phase, then the result obtain from this approach is used to generate the sliding mode control that ensures the robustness in the sliding phase of the variable structure control regarding disturbances, time delays and uncertainties. Also, a varying parameter is used to adapt "online" the robust control to the level of the disturbances in linear varying parameter strategy. The use of a discrete control approach allows faster, easier and more realistic result for the experimental implementations.

This paper is organised as follows: section 1 is devoted to introduce the aspects of design and control of the new proposed actuator. In section 2, the actuator design procedure is presented with specification requirements and parameter optimization. Section 3 presents the new control strategy proposed for the position control of the newly developed actuators. Section IV presents the simulation results in different scenarios that validates the developed control strategy for the designed actuator. Conclusions and some future works that have been already started are presented in last section.

2. DESIGN OF A NEW GENERATION FORCE FEEDBACK SIDESTICK FOR AIRCRAFT COCKPIT CONTROL

The objective of this work is to provide a new solution to enhance the aircraft's flight performances using a new design and control for sidesticks actuators considering the human factor interaction in loop. Indeed, the pilot behaviour can be influenced by the haptic sensations generated while controlling the flight surfaces (see Allias et al. (2014) and Bailey (1963)).

In this study, a new generation of the active sidestick sytem is developed to improve the haptic sensations and then the flight performance. This actuator is a double airgap synchronous permanent magnets machine with non-entire arc and a Halbach array pattern (see Fig 2) in order to provide more torque.

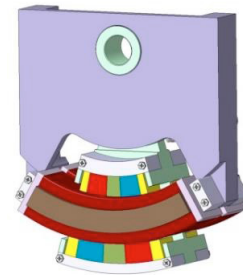To cope with the constraints and specifications that this

Fig. 2. Double airgap synchronous permanent magnets actuator

embedded aeronautical application requires, an optimization process is used.

2.1 Set of Specification requirements

The aeronautical application requirements must be respected in the design of the new actuator. Indeed, it implies a set of specifications that the design must comply with (dimensions, forces, strokes, speed, temperature and force ripples). Also, to respect the safety requirements, two identical actuators have to be implemented in parallel (security conditions impose redundancy over each one of the pitch and roll axes).

Usually, the effort of commonly used passive stick in the cockpit is linearly dependent to the input displacement angle while in this active case, the effort of the sidestick can be considered as a piecewise continuous function of the displacement angle as in Fig. 3.

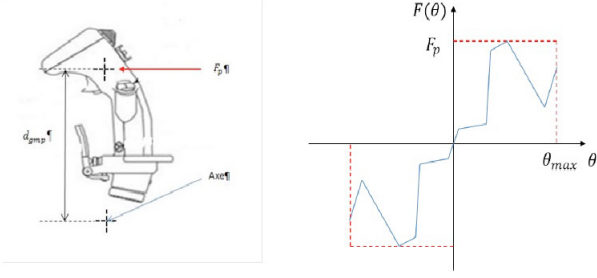One of the main characteristic of this system is the

Fig. 3. Force/Displacement angle characteristic

maximum torque provided by each one of the actuator. It depends on the grip middle point distance $d_{gmp}(seeFig.3)$. Then, the maximum torque to be developed is given by:

$$T_p = F_p * d_{gmp} = 3.2(Nm) \qquad (1)$$

where F_p is the force applied by the pilot on the sidestick. Then, in the design procedure the following specifications are to be considered (to respect the restrictions regarding the aeronautical application): It is important to take into

Table 1. Specifications for the designed actuator.

Parameters	Double airgap rotating machine
Torques (C_m Nm)	3.2
Force (F_p (daN)	2
Size box (mm^3)	$175 * 150 * 60$
Range of displacement ()	$[-15, 15]$

account these specifications to perform the optimization for the design procedure.

2.2 design structure

As previously presented, the new double airgap actuator is designed to be close to a classical permanent magnet machine. Indeed, more specifically it is can be considered as 1/12 of the PM machine. Then, it is important to reduce the rotor and stator opening angles (α_r and α_s respectively, see Fig. 4). This can be expressed as follows:
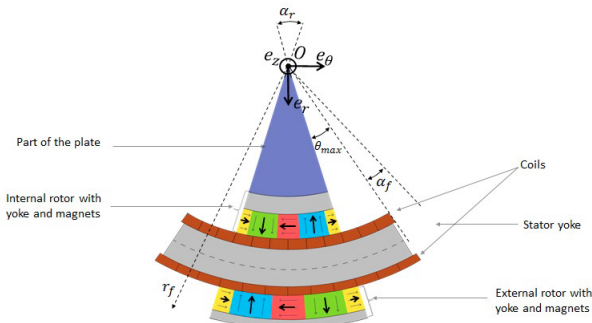

Fig. 4. Section view of the actuator

$$\begin{cases} \alpha_r \leq \alpha_s \\ \alpha_s = \alpha_r + \alpha_d \\ where \ \alpha_d \in [-\theta_{max}, \theta_{max}] \end{cases} \qquad (2)$$

Where θ is displacement angle of the actuator and θ_{max} = 15 (specification requirements).

Remark 2.1. It has to be noticed that in Fig. 4 the angle α_f is set to describe the part used to fix the stator in the containing box, and r_f is the radius of the machine. When performing the optimization, it is important to consider the obstruction of the actuators in the box (H_box, L_{box}, P_{box}). This can be analytically expressed in 3 as follows:

$$\begin{cases} r_f \leq H_{box} \\ \alpha_s = 2 * arcsin(\dfrac{L_{box}}{2 * r_f}) \\ 2 * (w + w_p + e_z + 2 * e_l) \end{cases} \qquad (3)$$
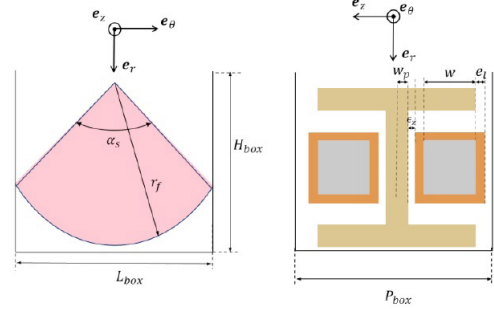

Fig. 5. Obstruction limitations

Also, the materials used to build this new sidestick are adapted to the aeronautical application. The magnets are in Samarium COb lt with a remanent polarization $\hat{J}$ of 116 (T) and a critical temperature around $165C$ (demagnetization). The yokes are in iron cobalt with lamination of $35mm$ on the stator yoke and without lamination on the rotor. A succession of coils (made of an epoxy resin supporting 140) and non magnetic wedges are arranged on the yoke as in Fig. 6. Because of the required high torques
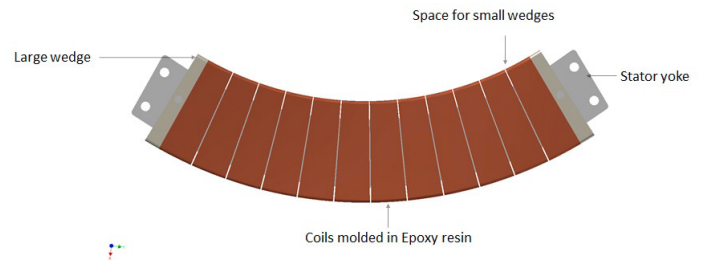

Fig. 6. Illustration of the machine coils

per unit of mass that must be provided by the actuator, a Halbach array magnetization for the magnets is used. It means that there is a combination between radial and tangential magnetization as in Fig. 7. It is worth noticing that each one of the coils is supplied by 3 phase sinusoidal current, the total torque developed by the each coil of the actuator is obtained by calculating the average of laplace force over a coil area (Allias et al. (2014)):

$$T_L^k(t) = \frac{1}{Scoil} \int_{scoil} \int_z B_y(\theta_s, Y, t).I^k(\theta_s, t).dz.dS \qquad (4)$$

Where S is the area of a slot (coil), B is the magnetic flux density, I is the electric current.
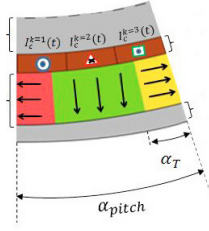
Fig. 7. Representaton of the machine coils Halbach array

Total torque for the rotating actuators, considering 3-phase sinusoidal current are:

$$T_m(t) = 2p \sum_{k=1}^{3} T_L^k \qquad (5)$$

where p is the number of pairs of pole, $k = 1, 2, 3$.
Let's recall that the pilot (using each one of the redundant actuator) has to be able to provide a maximum torque of 3.2 (Nm) for a maximum time laps that not exceeds 5 (mn).

2.3 Optimization of the actuator design parameters

The optimization is an important step in the design procedure to ensure to fit into the specific set of specification and to get the best design parameters required to the considered application .
The main objective for this actuator is to develop a high torque in a small volume. For this sake, a multi-objective function is used for the optimization, as follows:

$$\begin{cases} min f(x), \\ g_i(x) \leq 0, \forall i \in 1, ..., n_g \\ h_j(x) = 0, \forall j \in 1, ..., n_h \end{cases} \qquad (6)$$

where f is the objective function to minimize under the g_i and h_j constraints. x is the vector of the variables for the optimization and n_g and n_h are respectively the number of inequalities and equalities constraints.
The objective function is given as follows:

$$f(x)(t) = \sum_i \gamma_i \frac{f_i(x)}{||f_i||} \qquad (7)$$

with

$$\sum_i \gamma_i = 1 \qquad (8)$$

where γ_i is the weight given to each one of the mono-objective f_i. Indeed, the following objective functions are considered:

$$f_1 = -T_m \qquad (9)$$

$$f_2 = \eta = \frac{P_{em}}{P_{em} + P_{joule}} \qquad (10)$$

where η is the efficiency of the actuators. $P_{em} = T_m.\gamma$ is the electromagnetic power and P_{joule} is the Joule losses. Here, the eddy losses are not considered because the supply frequency is low ($< 10Hz$) du to the maximal rotating speed imposed by the specifications ($100/s$). This optimization is achieved thanks to the $MATLAB^{\circledR}$. Indeed, f_{mincon} function is used as the minimization function and the *Interior-point* algorithm. Also the *global-search* function is used since it is based on a multi-start method. After designing the actuator, a new control strategy is

Table 2. Optimized parameters of the designed actuator.

Parameters	New designed Rotating machine
Torques (Nm)	3.17
Mass (kg)	0.95
Torque per unit of mass	3.65

developed considering results in (see Table. 2) to achieved the desired tracking performances.

3. ROBUST OPTIMAL SLIDING MODE CONTROL DESIGN STRATEGY

The proposed control strategy is developed to achieve the desired performance objectives (good tracking, disturbances rejection, uncertainties, time delays). Since the considered actuator is a part of the whole cylindrical PMSM, the rotational motion of this actuators is in the rang [15, 15]. A position control of the rotative displacement of this actuator to generate the required torque must be achieved. The proposed discrete control strategy is based on an LQR control to shape the actuator dynamics (Zhou et al. (1996)) and then the resulting gain to generate the variable structure control based on the Sliding Mode (VADIM (1977)) for the robustness purposes. Also, the level of robustness to the disturbances is adapted "online" using a varying parameter based on the variation of the system inertia (main disturbance induced by the pilot inertia). This strategy is summarized in Fig. 8.
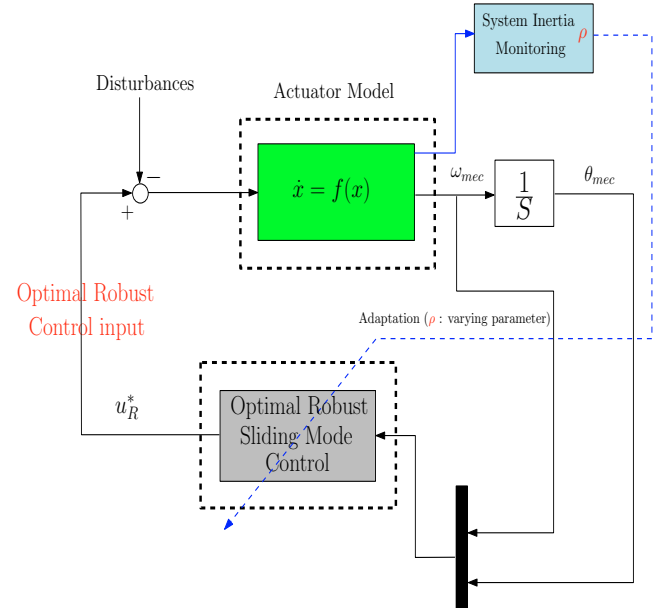

Fig. 8. Robust optimal actuator position control strategy.

3.1 Actuators model control-oriented

The considered PMSM actuators can be described by the following equations describing its rotation behaviour:

$$\begin{cases} v_d = L_d \dfrac{d}{dt} i_d + R_s i_d - \omega_s \phi_q \\ v_q = L_q \dfrac{d}{dt} i_q + R_s i_q - \omega_s \phi_d \end{cases} \qquad (11)$$

and

$$\begin{cases} \phi_q = L_q i_q \\ \phi_d = L_d i_d + \phi_m \ (avec \ \phi_m = L_m I_{mf}) \end{cases} \quad (12)$$

where, v_d, v_q are the $d,q-axes$ stator voltages, i_d, i_q are the $d,q-axes$ stator currents, L_d and L_q are $d,q-axes$ stator inductances, λ_q and λ_d are $d,q-axes$ stator flux linkages. Also, R_s and ω_s are the stator resistance and electric pulse while L_m and I_{mf} are the mutual inductance and the equivalent $d-axis$ magnetizing current.

The corresponding developed electromagnetic torque T_{elec} is given as follows:

$$T_{elec} = \frac{3}{2} p [L_m I_{mf} i_q + (L_d - L_q) i_q] \quad (13)$$

where p the number of pole pairs.

Then, the corresponding electromechanical equations are:

$$J_{mec} \frac{d\omega_{mec}}{dt} + B_{mec} \omega_{mec} = T_{elec} - T_{load}$$

$$\frac{d\theta_{mec}}{dt} = \omega_{mec} \quad (14)$$

where θ_{mec} and ω_{mec} are the mechanical position and velocity of the rotor. J_{mec} and B_{mec} are the moment of inertia and the damping coefficient respectively. The electrical frequency (inverter frequency) ω_s is related to the rotor velocity through $\omega_s = p\omega_{mec}$.

Remark 3.1.
- PMSM control is based on the control of field orientation since the magnetic flux is in relation with rotor position.
- T_{elec} is proportional to the controlled current i_q. The current i_d is fixed by the controller at null value.
- J_{mec} represents the moment of inertia created by both the sidestick and the motor, and then T_{load} represents the disturbances induced by the pilot handling of the sidestick.

3.2 System description

The transfer function that describes the previous system by considering a time delay is the following:

$$F(s) = \frac{1}{s} \left(\frac{1}{J_{mec} s + B_{mec}} \right) e^{-t_d s} \quad (15)$$

Remark 3.2. In this work, the delay can be generated by several causes as frictions, realizations constraints and experimental implementation procedures. A Smith predictor is used to model these delays.

The continuous time state model is then given as follows:

$$\begin{cases} \dot{x}(t) = Ax(t) + Bu(t - t_d) \\ y(t) = Cx(t) \end{cases} \quad (16)$$

Where $x(t)$ is 2×1 state vector, $A \in R^{2 \times 2}$, $B \in R^{2 \times 1}$ and $C \in R^{1 \times 2}$. $u(t)$ represents the control input which is the electrical torque developed by the actuator, $y(t)$ is the system output, and t_d is the considered time delay.

The discretization of this representation in Eq. 16, give the discrete-time state model as:

$$\begin{cases} x(k+1) = Gx(k) + Hu(k-d) \\ y(k) = Cx(k) \end{cases} \quad (17)$$

Where $G \in R^{2 \times 2}$, $H \in R^{2 \times 1}$, $C \in R^{1 \times 2}$ respectively represent discrete time state space martices and $x(k)$ is the discrete state vector and d is the number of the delay

samples.
G and H matrices in Eq. 19 are obtained as follows:

$$\begin{cases} G = e^{AT} \\ H = \left[\int_0^T e^{AT} dt \right] B \end{cases} \quad (18)$$

Where T represents the simple period.

Remark 3.3. One of the main advantage of using the **Hallbach** polarization is to shape the magnetic field flux to avoid the saturation on the motor borders (Ravaud et al. (2010)). Thus, only isolated points of saturation could appear while using the motor at maximum torque. This saturations are considered as disturbances of the nominal behaviour of the motor and will be managed by the proposed robust control structure.

3.3 Time delay prediction

To handle the delay, a delay ahead predictor is used. It is equivalent to the model with the Smith predictor and helps to simplify the controller synthesis. As in Mihoub et al. (2009), it is constructed by removing the delay form Eq. 19 as follows:

$$\begin{cases} x^*(k+1) = Gx^*(k) + Hu(k) \\ y^*(k) = Cx^*(k) \end{cases} \quad (19)$$

Remark 3.4. For implementation purposes and to handle the undesired disturbances and modeling errors, the following correction is achieved:

$$\begin{cases} \hat{x}_1(k+d \ k) = x_1^*(k) + y_{mes}(k) - x_1(k) \\ \hat{x}_2(k+d \ k) = x_2^*(k) \end{cases} \quad (20)$$

Where y_{mes} is the measured output of the actuator.

3.4 Robust control design

The proposed control synthesis scheme is based on shaping the motor dynamics through the introduction of a performance index and an LQR feedback gain stabilization. Then, a robust variable structure control based on sliding mode will conserve this performances in non nominal conditions. Also, an adaptation of the robustness level is provided using a varying parameter in an LPV context (Ballesteros and Bohn (2011)).

The aim of this control is to track a desired position of the PSMS based on the state space representation. First, an LQR optimal control is used to find an optimal input u^*, that minimizes the performance index:

$$J = \sum_0^\infty (x^{*T}(k) Q x^*(k) + u^{T(k)} Ru(k)) dt \quad (21)$$

where **R** is positive definite, and **Q** is nonnegative symmetric positive definite matrix.

The optimal control input u^* for the considered system is obtained by first computing the nonnegative solution $\bar{P}$ of the following Riccati equation (see Barabanov and Ortega (2004):

$$P = Q + G^T P [I + HR^{-1}H^T P]^{-1} G \quad (22)$$

Where P is positive definite real symmetric and I the identity matrices.

Then, the optimal feedback to be applied to achieve the

performance objective of the position tracking is the following:

$$K^* = 2R^{-1}H^T(G^T)^{-1}[P - Q] \quad (23)$$

This LQR optimal control is used to shape the dynamics of the motor to meet the required performance in the nominal case, but it may not be sufficient in case of disturbances or parameters uncertainties. Then to manage these problems, the following robust sliding mode control complementary strategy is introduced (Shyu and Shieh (1996)). A sliding surface (function $\sigma(x^*(k))$) for the sliding mode control position base on the LQR feedback defined in (23):

$$\sigma(x^*(k)) = K^*C^T\Big[(x^*(k) - x_d^*) - A_c\sum_0^T x^*(k)\Big] \quad (24)$$

where A_c is the closed loop dynamical matrix obtained using the LQR control in (23), K^* is the optimal controller previously presented in Eq. 23, x_d^* the desired state vector, C^T is chosen to fulfill the following condition: $C^T B \neq 0$, so it can meet the requirement of the sliding mode definition and simplify (24). A simple solution is $C^T = [0 \ 1/J_m]$. The input control that forces the system states ($\sigma(x^*(k + 1)) = 0$) to reach the sliding surface during all the process control as follows:

$$\Big\{ u_f(k) = (K^*C^TH)^{-1}(K^*C^TA_c\sum_0^{T-1} Gx^*(k) - K^*C^Tx_d^*) \quad (25)$$

Then, for the sliding part, a discontinuous function is used to ensure more robustness as follows:

$$u_{sld}(k) = \sigma(x^*(k))sign(\sigma(x^*(k))) \quad (26)$$

The new global control input u_R^* that allows that achieves the desired performances is given as follows:

$$\begin{aligned} u_R^*(k) &= u_f(k) + u_{sld}(k) \\ u_R^*(k) &= u_f(k) + \rho\sigma(x^*(k))sign(\sigma(x^*(k))) \end{aligned} \quad (27)$$

The sign function is quite rough since it is defined as:

$$sign(s(t)) = \begin{cases} +1 \ if \ s(t) > 0 \\ -1 \ if \ s(t) < 0 \end{cases} \quad (28)$$

Then to have smoother function and simplify the sliding optimal control implementation, the following robust control input is considered:

$$u_R^*(k) = u_f(k) + \rho\frac{\sigma(x^*(k)}{|\sigma(x^*(k) + \delta|} \quad (29)$$

where $\delta << 1$.
ρ is the varying parameter that adapt the level of robustness of the considered control strategy "on-line" to the total perturbation, as follows:

$$|\frac{pert}{B_{mec}}| \leq \rho \quad (30)$$

Where $pert$ is the level of disturbances that influence the system.
Several academical studies have shown that the pilot inertia is the main disturbances source that affect the behaviour of the active sidestick, mainly, changing the system inertia. Thus, the adaptation of the robustness of proposed controller is scheduled by the following varying parameter ρ, based on the variation of the system inertia:

$$\rho = \frac{|J - J_{nominal}|}{|J_{nominal}|} \leq 1 \quad (31)$$

where, J: is the system global inertia (affected by the pilot), $J_{nominal}$: the designed actuator inertia.

Remark 3.5. Using a varying parameter to adapt the level of rejection of the proposed robust control leads to a polytopic representation of two vertices of the control. Thus, the global dynamical LPV controller can be easily written in a convex polynomial combination of local controllers on the vertices of a polytop formed by the higher and lower bound of the variation interval of the varying parameter ρ.

Then, it is established that for any optimal LQR feedback (see (7)), the system has a switching surface (σ) on which the states slides.

stability proof of the discrete sliding monde control.
The previously proposed robust discrete sliding monde control for the actuator position is based on the sliding mode strategy. The control stability can be evaluated by choosing the following definite positive Lypunov function:

$$V(k) = |\sigma(x(k))| \quad (32)$$

Then

$$\Delta V(k) = |\sigma(x(k + 1))| - |\sigma(x(k))| \quad (33)$$

The stability condition is then that $|\sigma(x(k + 1))| \leq |\sigma(x(k))|$. This reaching condition of the discrete sliding monde control is obtained using Eq. 24 to Eq. 29, and Eq. 35:

$$|K^*C^THu_{sld}(k)| - |\sigma(x(k))| \leq 0 \quad (34)$$

Which leads to the following condition:

$$|K^*C^THu_{sld}(k)| \leq |\sigma(x(k))|$$

$$|K^*C^TH| < 1 \quad (35)$$

Remark 3.6. For the experimental implementation, the delay ahead predicted states are replaced by the corrected states (based on the real measurements) in the proposed control strategy as in Eq.20.

4. SIMULATION RESULTS

The following simulations are performed to test the efficiency of the proposed control strategy. The main objective of this control is to achieve the best position tracking performances that allow to enhance the pilot control of aerodynamical surfaces of the aircraft.
. First, the objective is to control the position of the motor in **nominal** conditions for the considered angles range of variation (-15 to $+15$).
To emphasize the reliability of the control strategy, a comparison between the classical LQR control, the Camacho et al sliding mode control strategy (see Camacho and Smith (2000)) and the proposed sliding mode combined LQR control is presented to evaluate the performances. The following scenario concerns a position tracking of $0.261rad$ (15) with a time delay $t_d = 0.05$. A step signal is applied to the system to validate the efficiency of the proposed strategy at $t = 0$. Fig. 9 shows the portion tracking control for the new designed actuator in nominal conditions. It can be seen that the response produced by the proposed control strategy is faster then the one given by the classical LQR controller or Camacho et al sliding controller. Also, it is smoother than the others controllers. Indeed, even
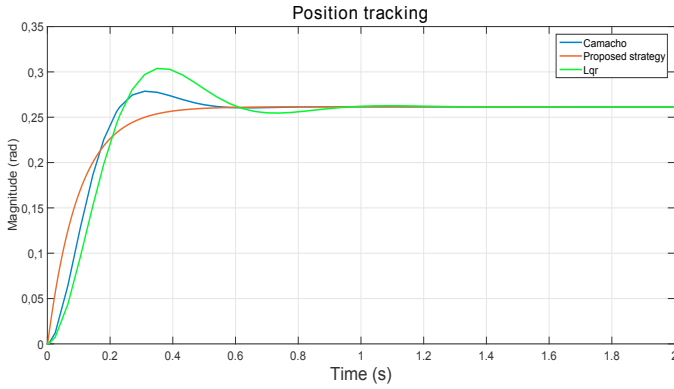
Fig. 9. Position tracking control .

with a good time response obtained with Camacho et al controller, one can see that it produces a heavy overshoot. Fig. 10 shows that the new developed controller allows to
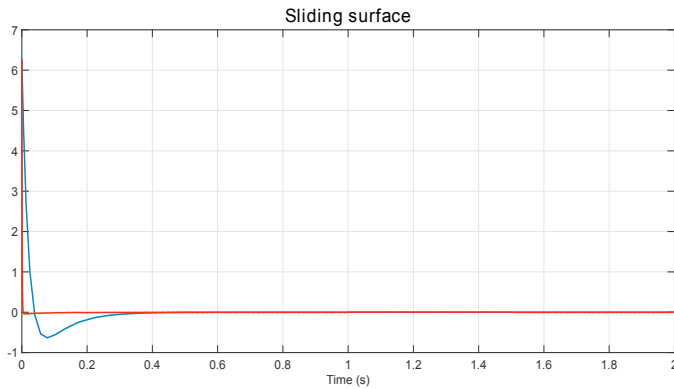

Fig. 10. Sliding surface .

reach faster the sliding surface compared to Camacho et al sliding control strategy. Indeed, this will provide more robustness and enhance the performances of the system thanks to the time reduction of the reaching phase Utkin et al. (1993).

The next scenario concerns the position control of the actuator in disturbed conditions (uncertainties and external disturbances). This simulation allows to test the robustness and the proposed solution by considering a parametric uncertainty level of 25% to overall time constants of the system. Also, at $t = 0.4$ the system is subject to a significant disturbance signal (tracking reference if a step signal of 0.261 rad (15)). In Fig. fig:distrubsld, a
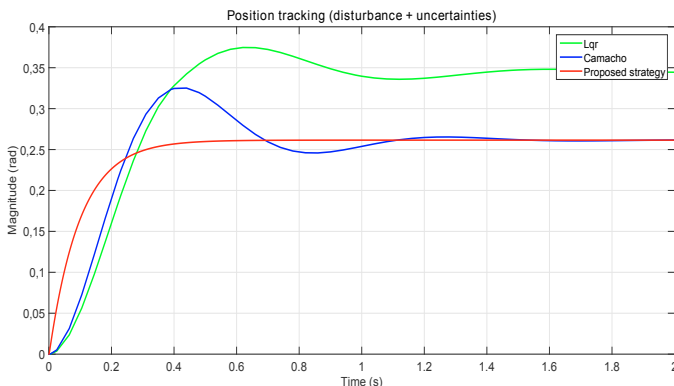

Fig. 11. Position control: disturbed conditions..

camparaison between the proposed control strategy, the Camacho et al controller and the LQR controller. It can be seen that the LQR controller can not handle the uncertainties and fail to reject the disturbance on the system. The Camacho et al sliding control manage to converge to the desired position but after a long time and with cost of heavy overshoots. The proposed control solution manages to handle the uncertainties and the reject the disturbance thanks to the adaptive optimal sliding control structure and provides satisfactory results.

Remark 4.1. The proposed optimal sliding mode strategy is very robust to the disturbances. The sliding control allows to keep the performance objective and to reject all the disturbance instantaneously by stabilizing the states of the system in the "sliding phase". Then, ensures a robust optimal control from the beginning of the process.

The *RMS* (Root Mean Square value) of the position tracking error signals allows compare these strategies. For the proposed robust control strategy, the *RMS* of the tracking error is of 1.2% while for the Camacho et al controller the *RMS* of the error is of 21%. This proves the efficiency of the proposed strategy.

5. CONCLUSIONS AND FUTURE WORK

In this work, a design of novel sidessidestick electromagnetic actuator for aeronautical application have been presented (a patter has already been validated). The design procedure have been introduced and more details (using specific softwares and step by step design procedure and optimization can be found in authors works in Allias (2015). Then, a new discrete robust adaptive sliding mode control strategy that allows to enhance the position tracking regarding the aeronautical application requirements, and to handle the time delay, uncertainties and the disturbances on the system.

Simulation results using the designing parameters and comparison with the classical optimal control (LQR) and the Camacho et al sliding mode controller proves the efficiency of the described approach for the considered application.

The next step is implementing the developed strategy. Indeed, the experimentation phase has been decided to be achieved in two steps: a test-bed developed in the laboratory to start testing the design and control structures as shown in Fig. 12. The next step is to realize the new
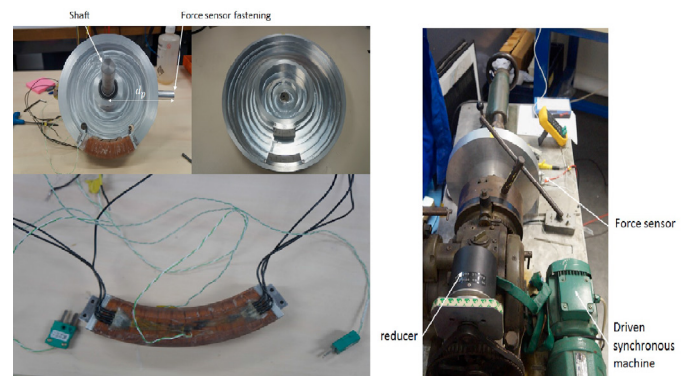

Fig. 12. Preliminary test bed for experimentation.

designed actuator with the the embedded control unit for

civilian aircraft which is one of the objectives of the French National Research Agency TEMOP.

REFERENCES

Adams, R.J., Buffington, J.M., Sparks, A.G., and Banda, S.S. (2012). *Robust multivariable flight control*. Springer Science & Business Media.

Allias, J. (2015). *DIMENSIONNEMENT D'UN ACTIONNEUR POUR ORGANE DE PILOTAGE A ENTRAINEMENT DIRECT AVEC REDONDANCE PASSIVE MAGNETIQUE*. Ph.D. thesis, Universite Paul Sabatier, Toulouse, France.

Allias, J., Llibre, J., Henaux, C., Briere, Y., and Alazard, D. (2014). A global approach for the study of forces developed by a tubular linear moving magnet. In *Electrical Machines (ICEM), 2014 International Conference on*, 2654–2660. doi:10.1109/ICELMACH.2014.6960563.

Bailey, A. (1963). Developement of a side stick controller for aerospace vehicles. *Honeywell Aeronautical Division, Minneapolis, MN*.

Ballesteros, P. and Bohn, C. (2011). Disturbance rejection through lpv gain-scheduling control with application to active noise cancellation. In *Proceedings of the IFAC World Congress*, 7897–902.

Barabanov, N.E. and Ortega, R. (2004). A note on extended algebraic riccati equations appearing in dissipativity theory. In *Robust Control Design 2003 (ROCOND 2003): A Proceedings Volume from the 4th IFAC Symposium, Milan, Italy, 25-27 June 2003*, 13. Elsevier Science Limited.

Bhattacharyya, S., Chapellat, H., and Keel, L. (1995). Robust control: the parametric approach. *Upper Saddle River, New Jersey*.

Brière, D. and Traverse, P. (1993). Airbus a320/a330/a340 electrical flight controls-a family of fault-tolerant systems. In *Fault-Tolerant Computing, 1993. FTCS-23. Digest of Papers., The Twenty-Third International Symposium on*, 616–623. IEEE.

Camacho, O. and Smith, C.A. (2000). Sliding mode control: an approach to regulate nonlinear chemical processes. *ISA transactions*, 39(2), 205–218.

Carriere, S., Caux, S., and Fadel, M. (2010). Optimised speed control in state space for pmsm direct drives. *IET electric power applications*, 4(3), 158–168.

Gandhi, N., Richards, N., and Bateman, A. (2014). Simulator evaluation of an in-cockpit cueing system for upset recovery. In *AIAA Guidance, Navigation, and Control Conference*.

Hanke, D. and Herbst, C. (1999). Active sidestick technology–a means for improving situational awareness. *Aerospace science and technology*, 3(8), 525–532.

Hegg, J.W., Smith, M.P., Yount, L., and Todd, J. (1995). Features of active sidestick controllers. *Aerospace and Electronic Systems Magazine, IEEE*, 10(7), 31–34.

Karpenko, M. and Sepehri, N. (2009). Hardware-in-the-loop simulator for research on fault tolerant control of electrohydraulic actuators in a flight control application. *Mechatronics*, 19(7), 1067–1077.

Kumar, M.V., Sampath, P., Suresh, S., Omkar, S., and Ganguli, R. (2008). Design of a stability augmentation system for a helicopter using lqr control and ads-33 handling qualities specifications. *Aircraft Engineering and Aerospace Technology: An International Journal*, 80(2), 111–123.

Lam, T., Mulder, M., and Van Paassen, M. (2008). Haptic feedback in uninhabited aerial vehicle teleoperation with time delay. *Journal of guidance, control, and dynamics*, 31(6), 1728–1739.

Mihoub, M., Nouri, A.S., and Abdennour, R.B. (2009). Real-time application of discrete second order sliding mode control to a chemical reactor. *Control Engineering Practice*, 17(9), 1089 – 1095.

MORGAN, J. (1991). An initial study into the influence of control stick characteristics on the handling qualities of a fly-by-wire helicopter. *AGARD, Flying Qualities 13 p(SEE N 91-23108 15-05)*.

Navarro, R. (1997). *Performance of an electro-hydrostatic actuator on the F-18 systems research aircraft*. National Aeronautics and Space Administration, Dryden Flight Research Center.

Ravaud, R., Lemarquand, G., and Lemarquand, V. (2010). Halbach structures for permanent magnets bearings. *Progress In Electromagnetics Research M*, 14, 263–277.

Shyu, K.K. and Shieh, H.J. (1996). A new switching surface sliding-mode speed control for induction motor drive systems. *Power Electronics, IEEE Transactions on*, 11(4), 660–667.

Utkin, V. et al. (1993). Sliding mode control design principles and applications to electric drives. *Industrial Electronics, IEEE Transactions on*, 40(1), 23–36.

VADIM, I.U. (1977). Survey paper variable structure systems with sliding modes. *IEEE Transactions on Automatic control*, 22(2).

Wyllie, C. (1988). Aircraft side hand controllers-where to from here ? In *Aerospace and Electronics Conference, 1988. NAECON 1988., Proceedings of the IEEE 1988 National*, 454–460. IEEE.

Zanlucchi, S., Masarati, P., and Quaranta, G. (2014). A pilot-control device model for helicopter sensitivity to collective bounce. In *ASME 2014 International Design Engineering Technical Conferences and Computers and Information in Engineering Conference*. American Society of Mechanical Engineers.

Zhou, K., Doyle, J.C., Glover, K., et al. (1996). *Robust and optimal control*, volume 40. Prentice hall New Jersey.